

Video Observation of Waves and Shoreline Change on the Microtidal James Town Beach in Ghana

Donatus B. Angnuureng^{†*}, Rafael Almar[‡], Kwasi Appeaning Addo[§], Bruno Castelle[†], Nadia Senechal[†], Sowah W. Laryea[§], George Wiafe[§]

[†]UMR EPOC, University of Bordeaux / CNRS, Bordeaux, France.

[‡]IRD/UMR, LEGOS, Toulouse, France.

[§]MAFS/Remote Sensing Lab., University of Ghana, Accra, Ghana.



www.cerf-jcr.org



www.JCRonline.org

ABSTRACT

Angnuureng, D. B., Almar, R., Appeaning Addo, K., Senechal, N., Castelle, B., Laryea, S. W., Wiafe, G., 2016. Video observation of waves and shoreline change on the microtidal James town Beach in Ghana. *In: Vila-Concejo, A.; Bruce, E.; Kennedy, D.M., and McCarroll, R.J. (eds.), Proceedings of the 14th International Coastal Symposium (Sydney, Australia). Journal of Coastal Research, Special Issue, No. 75, pp. 1022 – 1026, Coconut Creek (Florida), ISSN 0749-0208.*

The morphology of sandy beaches is highly dynamic. They are influenced by the geology of the coastal area and external hydrodynamic forcing. On long timescales (years to decades), it is more efficient and convenient to monitor beach evolution through remote sensing technics rather than through direct field measurements. Erosion is a major problem along the coastline of Ghana with over 25 erosion hotspots, including James town. Here, tides, ECMWF EraInterim re-analysis wave data and images covering the beach area have been obtained for the 2013-2014 period. This paper presents preliminary results of the first efforts in processing video-derived observations of waves and shoreline change in Ghana. The pilot application shows a strong potential of the video system in providing fair quality wave data for beach management purposes where video wave characteristics are in good agreement with EraInterim global reanalysis (daily RMSE = 0.8 m and 0.7 m for H_b and T_p , respectively). Shorelines extracted from video suggest large monthly variability driven by wave seasonality while shoreline change shows a subsequent erosion/accretion cycle.

ADDITIONAL INDEX WORDS: *Shoreline location, wave modeling, beach profile changes.*

INTRODUCTION

Understanding coastal processes in the nearshore at different time scales is crucial, especially in the present context of vulnerability to sea level rise (Sagoe-Addy and Appeaning, 2013; Stive *et al.*, 2002). Vulnerability of beaches to natural forcing and anthropogenic factors has been addressed through both hard (*e.g.* revetments, jetties or breakwaters, and groins (Angnuureng *et al.*, 2013)) and soft (*e.g.* revegetation and beach nourishment) approaches in attempts to control the changes (*e.g.* French, 2001; Turner and Leatherman, 1997) yet both methods are debatable. Traditionally, studies in the nearshore have been realised via topographic surveys and in-situ measurements (Stockdon and Holman, 2002). However these measurements are intermittent both in space and time and the distance covered is often limited. The nearshore is a very variable system constantly changing at various timescales (Puleo *et al.*, 2003) and require a high frequency of sampling for adequate characterization. Remote video imagery has been used to measure nearshore processes (*e.g.* Aarninkhof *et al.*, 2003; Armaroli and Ciavola, 2011; Holman and Stanley, 2007; Plant and Holman, 1997) over the past two decades. According to Holman and Stanley (2007), the video system gives good resolutions (cm to m), and is safe and cheap.

From video images, wave height, celerity and period (*e.g.* Almar *et al.*, 2008; Holman and Stanley, 2007); break point and intertidal sandbar locations (Holman and Stanley, 2007; Ruessink *et al.*, 2007), beach profiles, and shoreline position (Almar *et al.*, 2012a; Smith and Bryan, 2007; Plant and Holman, 1997) can be remotely estimated.

Along the Ghanaian coast, erosion has been observed to be increasing over the last decades (Appeaning Addo *et al.*, 2008; Boateng *et al.*, 2009) with over 25 erosion hotspots identified. On the eastern part, this is due to the method of management (*e.g.* groynes and revertment) which affects the sediment budget (Jayson *et al.*, 2013; Ly, 1980). Angnuureng *et al.* (2013) observed that erosion has increased from about 3 to about 17 m/yr. from 2001 to 2011, which has been probably enhanced by sand mining along the coast.

Monitoring of the Ghanaian coastline is mainly done using satellite images albeit rough resolution, aerial photographs and field observation using DGPS on an irregular basis. Though portions of the unmonitored coast remains, a well planned and reliable monitoring scheme with such methods does not guarantee the capture of the short term temporal shoreline evolution. It is then essential for the data gathering strategy to include events in all times and space, that such video system provides.

In the methods section, the James town study area is described and daily nearshore measurements from video imagery presented. The goal is to analyse the shoreline

DOI: 10.2112/SI75-205.1 received 15 October 2015; accepted in revision 15 January 2016.

*Corresponding author: angnuureng@yahoo.com

©Coastal Education and Research Foundation, Inc. 2016

evolution and the potential of the video system in providing fair quality wave data for beach management purposes.

METHODS

Shoreline and beach profiles were automatically extracted from the timex (or averaged) images and shoreline positions resampled into daily and 15-day values. The shoreline location can be obtained using various definitions (Boak and Turner, 2005) but here the procedure followed minimum shoreline variability (MSV) video technique (Aarninkhof *et al.*, 2003; Almar *et al.*, 2012a). Wave properties (e.g. breaker wave height H_b and peak wave period T_p) at breaking are extracted from video images to compare with hindcast wave data (WAM model, The Wamdi Group, 1988).

Study area

James town is a major fishing community in Ghana (Gulf of Guinea, West Africa) on the eastern part (Figure 1) of the Korle lagoon, which is a major ecological site in Accra under the Ghana wetlands management project. The shoreline erosion in Ghana has risen from 1.13 m/yr. (Appeaning Addo *et al.*, 2008) to a rate of about 2 m/yr. (Wiafe *et al.*, 2013). The increasing coastal erosion threatens the community, the lighthouse and the old Accra harbor presently being used as a fishing harbor.

The nearshore bathymetric profile is relatively gentle (Sagoe-Addy and Appeaning Addo, 2013) and the area experiences periodic high-wave conditions (e.g. Sagoe-Addy and Appeaning Addo, 2013). The mean wave incidence is SSW, mean peak period T_p and the mean significant wave height are 10.9 s and 1.4 m (Angnuureng *et al.*, 2013; Appeaning Addo *et al.*, 2008), respectively, but these could periodically rise to 20 s and 3 m. Tide range is micro-tidal with mean value of 1 m. Oblique waves drive alongshore drift of about $2 \times 10^5 \text{ m}^3/\text{yr}$. (Wellens-Mensah *et al.*, 2002) on this gentle beach (slope < 0.03).

The 40-m high lighthouse was built in the for navigation (insert, Figure 1). A video camera was mounted on the lighthouse on 14/09/2013, inclined to the beach at an angle of 20° covering about 1.3 km across shore and 2 km along shore and recording from 6 - 18 hours GMT at 2 Hz. Three kinds of images are collected every 15 min: snapshot (Figure 2a); time exposure (timex) (Figure 2b) and time stacks (Figure 2c). Timex images are 15 min averaged of snapshot images into a single image (Almar *et al.*, 2012b; Holland *et al.*, 1997) while timestacks are obtained by stack of single cross shore section. The origin of the coordinate system (cross-shore $X=720$, longshore $Y=0$) is the lighthouse.

Geo-rectification of oblique images to plan view

Seven ground control points on site (Figure 2b, red circles) were taken with GPS and converted to Universal Transverse Mercator, UTM (Easting and Northing) coordinates. Including camera location (5.5265, 0.2121) at 30 N UTM zone, images were geo-rectified from oblique to plan view images by applying the method of direct linear transformation (e.g. Argus, Holland *et al.*, 1997). To get the rectified data, two approaches were applied. First, a zone of interest covering the beach and water (Figure 2a, white patch) was selected on the image and rectified at a 1-m resolution before desired information was extracted. We used for the rectification, the focal length (4m)

based on a least square error minimization method. For shorter processing time purpose, the shorelines were detected (*see next section*) on the oblique images before the rectification.

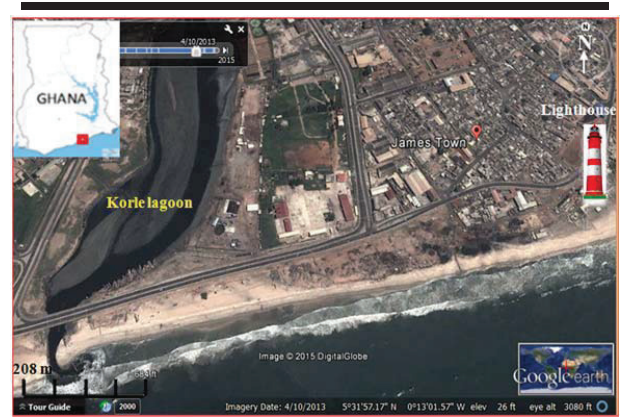


Figure 1. James Town Beach. Camera is mounted on lighthouse.

Because of the oblique camera view angle, the pixel resolution at the shoreline for the image lateral edges can be about 0.5 m, whereas it is about 0.1 m at the lower beach in front of the video system (Almar *et al.*, 2012a), increasing to 1 and 2 m at the lateral edges.

Automated shoreline delineation

Following Almar *et al.* (2012a), a region of interest (ROI) is demarcated on the oblique images to cover both wet (sea) and dry (land) pixels. Beach pixels display high red-channel values and low green values giving high $R:G$ ratio, whereas water pixels exhibit strong green-channel values and low red values (i.e. low $R:G$). Within the ROI (*see* Figure 2a), the $R:G$ ratios are computed for all pixels. These low and high values of $R:G$ mark water and beach respectively based on some bimodal distribution (Almar *et al.*, 2012a). The local minimum stands for the transition between water and beach, that is, the shoreline. In other words the shoreline is represented by the time averaged waterline. Figure 2b shows the location of the shoreline X delineated automatically. This was repeated for all images, and converted to metric values. To reduce uncertainties, a 1-hr moving average (4 points) was done. The overall error (0.5m) rises from water level uncertainties due to wave breaking or atmospheric pressure variations or wrong shoreline detection. 2D shoreline migration was estimated via the alongshore averaged cross-shore 2D location $\langle X \rangle$ (Figure 2c). 3D shoreline behaviour (non-uniformities development) was estimated through the standard deviation of cross-shore location along Y .

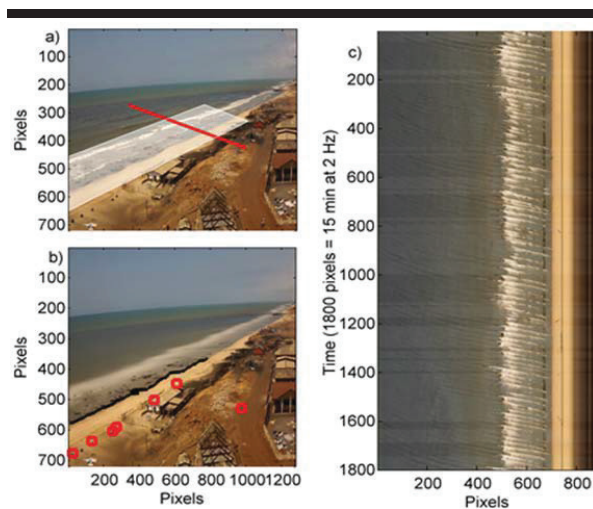


Figure 2. Video image types: a) snapshot; selected zone is shaded white while timestack profile is red line b) timex: shoreline is shown black line and GPS points in red circles c) timestack (vertical is time (1800 pixels = 15 min at 2 Hz).

Wave and tide data from models

To validate video estimates of wave properties, hindcast data of significant wave height H_s , direction and peak period T_p have been obtained from EraInterim global reanalysis (WAM model, The Wamdi Group, 1988) at 0.5° and 6 hr spatial and temporal resolution, respectively (Sterl and Caires, 2005) at the grid point 30°N , 30°W . The wave data spans from Sep. 2013 to Oct. 2014. Tide was extracted from WXTide model. Because there is no tide gauge at the study site, the tidal subordinate at Accra ($0^\circ 12' \text{W}$, $5^\circ 32' \text{N}$), from the nearest tide gauge station, Takoradi ($\sim 200 \text{ km}$) was used as the reference point. H_s and T_p were transformed into breaker conditions $H_{b(lm)}$ and $T_{p(lm)}$, respectively, following Larson *et al.* (2010). Beach states were computed using the formulation of Dean parameter (*see* Wright and Short, 1984), $\Omega = H_{b(lm)} / T_{p(lm)} w_s$, where w_s is sediment fall velocity, using the reanalysed wave data. A w_s of 0.05 m/s was used in consistence with similar sandy beaches (*e.g.* Masselink *et al.*, 2009).

Wave characteristics from video images

Wave breaker height H_b and T_p were obtained from time stack images and compared to the model data. T_p was computed from the offshore pixel intensity timeseries using mean zero-crossing method (Almar *et al.*, 2008). Following the wave signature induced by breaking, sudden variation in intensity values were identified on the image. For each breaker, standard deviation δ of the pixel intensity time series is estimated on a time window about the break point time. Almar *et al.* (2012b) showed that the width of the peak of δ marks the horizontal projection of wave face covered by the roller (L) which is subsequently projected into vertical H_b , $H_b = L \tan \beta$, where β is the camera view angle. H_b is obtained as the wave height of the average of all passing breakers over the timestack duration (1800s or stacking).

H_b and T_p were respectively regressed with $H_{b(lm)}$ and $T_{p(lm)}$, propagated from deep water to the breakpoint and a relationship established. Breaker parameters H_b and T_p from video followed this relationship.

Beach types were assessed from timex images. To estimate the beach profile evolution, 3D data (x, y, z) is needed. The shoreline location constitute 2D (x and y) which means a third axis (z -elevation) is needed. Subsequently profiles (not shown) were inferred from interpolated tide values at the different shoreline times where the profile of the beach at each time follow the tide values. The monthly average profiles were then estimated.

RESULTS

Preliminary findings of this West Africa pilot video system are given in the following subsections. They include the validation of video-derived wave parameters (RMSE, correlation with hindcast) and a brief description of the temporal evolution, extraction of shoreline and slope linked to wave and then tide forcing.

Validation of vide-derived wave characteristics

Figure 3 represents H_b and T_p obtained from regressed video-derived values as a function of hindcasted ones $H_{b(lm)}$ (and modelled $T_{p(lm)}$) from transformation of H_s , *see method section* following Larson *et al.* (2010). Figure 3a shows that corrected video-derived T_p correlates strongly with hindcast ($r = 0.9$, daily RMSE = 0.7). Result error is due to variation in image quality. In Figure 3b it is showed that corrected video-derived H_b is in agreement with $H_{b(lm)}$ ($r=0.9$, daily RMSE=0.8). Overall, these results show the reasonable skills of the video in estimating wave conditions from daily to monthly scale for this beach.

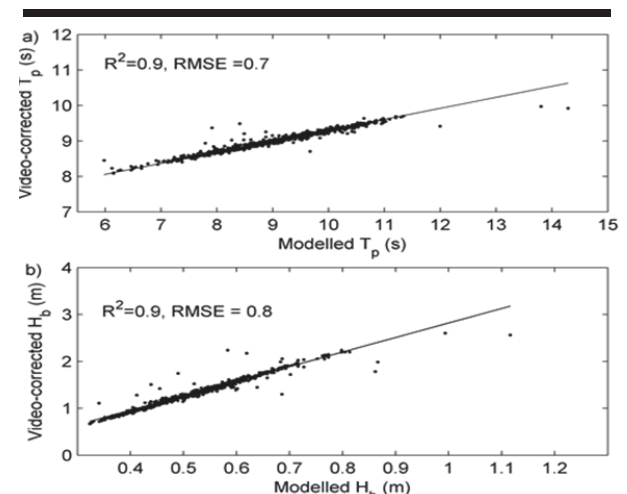


Figure 3. Time series a) corrected T_p from video values against model T_p b) corrected H_b from video values against model H_b . Model values are Larson's model H_b and T_p . Sloping solid lines are the best linear fits.

Shoreline and morphological evolution: event and overall evolution

During the observation period, from Sep. 2013 to Jul. 2014, alongshore averaged shoreline positions $\langle X \rangle$ ranged from 127 to 211 m with an average at 151 m. Figure 4c gives the daily $\langle X \rangle$ relative to the initial position $\langle X_i \rangle$. It shows that shorelines retreat beyond the $\langle X_i \rangle$ more than they advance. Shoreline alongshore non-uniformity $\Delta(X)$, i.e., standard deviation of shoreline X , is 8 m on average due to the presence of cusped pattern but can fall to 3 m during energetic conditions. H_b ranges from 0.3 to 2.5 m while literature reported between 0 and 2.8 (Angnuureng *et al.*, 2013). T_p ranges from 7 to 14 s at the zero mean crossing shown on the images. Figure 4d shows that H_b decreases from September, 2013 to January, 2014 concomitant to beach advance while after January, 2014, H_b increases progressively corresponding to shoreline recession till June, 2014. In Figure 4c, 15-day averaged shoreline positions are shown; September to early November period recorded beach advance gradually till it peaks in January. Shoreline retreats from January onward (Austral winter) when waves averagely become larger (Figure 4d).

Daily waves (H_b and T_p) did not correlate with shoreline positions as beach morphologies do not respond instantaneously to the changing wave field. Interestingly, similar results were found at a nearby beach (Grand Popo, Bénin) where the short term evolution of the shoreline seems to be more affected by tidal cycles from neap to spring (Bahini, 2015). This is due to the large Relative Tide Index (Masselink and Short, 1993) value which is around 1, even though the environment is microtidal. On the other hand, at the event scale, waves have more influence on $\Delta(X)$ development. $\Delta(X)$ is observed to correlate significantly at 95% ($p = 0.03$) with H_b though with low value ($r \sim 0.16$).

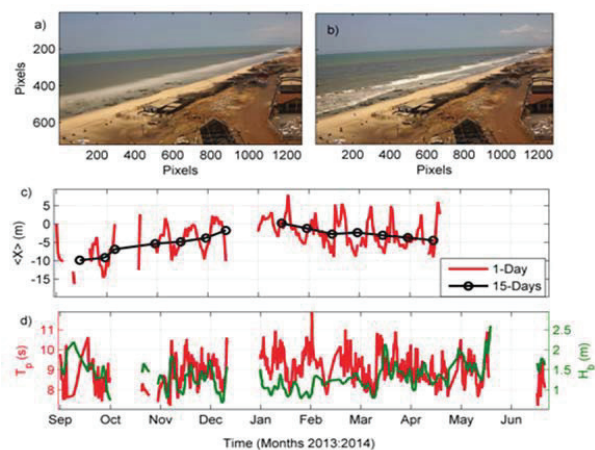


Figure 4. a) Timex b) Snapshot c) Daily (4 point moving average) and 15-Day shoreline locations $\langle X \rangle$ relative to the initial position $\langle X_i \rangle$ d) estimated H_b and T_p from video.

At the monthly scale, waves showed large correlation ($r = 0.87$) with $\langle X \rangle$ and $\Delta(X)$ than tides, TR ($r = -0.57$). This suggests waves have a strong influence on the shoreline location at seasonal scale. $\langle X \rangle$ correlates with alongshore non-

uniformity ($r = 0.3$, significant at 95%) which means errors in $\langle X \rangle$ decrease with decrease in its values. Though it is too early to conclude, a preliminary recessive change of the beach is envisaged. This is in line with previous studies (Appeaning Addo *et al.*, 2008) who observed an erosion of 1.13 m/yr. along the Accra Coast. Mean beach slope of 0.03 from tides against the horizontal shoreline positions indicates dissipative characteristics based on Wright and Short (1984) classification.

Noteworthy, video-derived beach slopes showed seasonal changes that can be attributed to an adaptation to wave energy modulation: with Ω ranging from 2 (intermediate beach state) in summer to 5 (dissipative) in winter, with steeper and gentle slopes in summer and winter periods

Beach profiles are estimated over a distance of 500 m from camera location and seaward. However, the estimation of topography from video at James town should be further validated using field measurements in order to get more confidence and robust conclusions on beach state evolution and variability.

DISCUSSION AND CONCLUSIONS

On a Ghana coastline of over 550 km presenting a large diversity (embayed and open beaches, sandbarriers, rivermouths) with recurrent shoreline problems, this is the first video system that has been used to continuously collect information on nearshore waves and beach changes.

The predictions of the H_b and T_p from video images and hindcast data are in good agreement, with RMSE of 0.7 and 0.8, respectively. This highlights the accuracy of the video in estimating waves parameters. Shoreline changes at James town show a seasonal response to waves with accretion during the austral summer months (Nov-Jan) and retreat during the winter months. The link between short-term shoreline evolution and waves conditions is less clear, as found at Grand Popo beach, Benin (Bahini, 2015) where short term evolution is attributed to tidal modulation. Overall, beach profile is in more dissipative state than predicted by Wright and Short (1984) classification with the absence of intertidal sandbars as one might expect. Although small, the variability of the beach profile is detectable. The results of the beach profiles show minor features probably due to the presence of small rocks observed around the study area. These rocks are well exposed on the images during low tides.

Beach and shoreline change analysed using video data covering 11 months suggest that breaking wave conditions and intertidal beach morphology can be continuously monitored. The results are consistent with previous findings though we suggest that large number of images be taken to give large seasonal shoreline data and minimise errors. Video deriving wave characteristics and shoreline change from a long-term monitoring perspective proved to be doable along this Ghanaian beach.

ACKNOWLEDGMENTS

The authors give appreciation to the French institute of research for development (IRD), the Office of Naval Research (US-ONR) project and Ghana ports and Harbour Authority for their support and also grateful to Benjamin Okyere, Alexander Boateng, Agbemebiase Nunana and Wilson Ako for their

assistance. This research has received support from French grants through French INSU/CNRS EC2CO-LEFE/IRD and ANR (COASTVAR: ANR-14-ASTR-0019).

LITERATURE CITED

- Aarninkhof, S.G.J., Turner, I. L., Dronkers, T. D.T. , Caljouw, M., and Nipius, L., 2003. A video-based technique for mapping intertidal beach bathymetry. *Coastal Engineering*, 49, 275–289.
- Almar, R., Ranasinghe, R., Catalan, P. A., Senechal, N., Bonneton, P., Roelvink, D., Bryan, K. R., Marieu, V., and Parisot J. P., 2012a. Video-based detection of shorelines at complex meso-macro tidal beaches. *Journal of Coastal Research*, 28(5), 1040-1048.
- Almar R, Cienfuegos R, Catalan PA, Michallet H, Castelle B, Bonneton P., and Marieu V., 2012b. A new breaking wave height direct estimation from video. *Coastal Engineering*, 61, 42-48.
- Almar, R., Senechal, N., Bonneton, P., 2008. Wave celerity from video imaging: validation with in-situ Pre-ECORS data. *Proc. I. C. C. E. I* (5), 661–673.
- Angnuureng, D.B., Almar, R., Senechal, N., Castelle, B., Appeaning Addo, K., Marieu, V., and Ranasinghe, R., 2015. Shoreline evolution under sequences of storms from video observation at a meso-macrotidal beach. *Geomorphology with major revision*.
- Angnuureng, B. D., Appeaning Addo, K., and Wiafe G., 2013. Impact of sea defense structures on downdrift coasts: The case of Keta in Ghana. *Academia Journal of Environmental Sciences* 1(6), 104-121.
- Appeaning Addo, K., Walkden, M., and Mills, J. P., 2008. Detection, Measurement and Prediction of Shoreline Recession in Accra, Ghana. *ISPRS Journal of Photogrammetry and Remote Sensing*, 63(5), 543-558.
- Armaroli, C., and Ciavola, P., 2011. Dynamics of a nearshore bar system in the northern Adriatic: A video-based morphological classification. *Geomorphology*, 126(1), 201-216.
- Bahini, A., 2015. Etude par imagerie video de la reponse du Littoral de grand popo benin de 2013 a 2015. Implications pour la stabilite de la plage. CIPMA-Chaire UNESCO, Université d'Abomey-Calavi, M.Sc. Thesis, 21p.
- Banno, M., and Kuriyama, Y., 2012. Multiple regression analysis of effects of bar and tide on shoreline change. *The Port and Airport Research Institute*, Kanagawa, 3-1-1, 239-0836.
- Boak, E.H., and Turner, I.L., 2005. Shoreline Definition and Detection: A Review. *Journal of Coastal Research*, 21(4), 688–703.
- Boateng, I., 2009. Development of Integrated Shoreline Management Planning: A Case Study of Keta, Ghana. *Paper presented at the FIG Working Week 2009*.
- French, W. P., 2001. Coastal Defences: Processes, Problems and Solutions. *Psychology Press*, pp 5.
- Holman, R.A., and Stanley, J., 2007. The history and technical capabilities of Argus. *Coastal Engineering*, 54, 477 – 491.
- Jayson-Quashigah, P. N., Appeaning Addo, K., and Kufogbe, S.K., 2013. Shoreline monitoring using medium resolution satellite imagery, a case study of the eastern coast of Ghana. *Journal of Coastal Research*, 65, 511-516.
- Ly, C. K., 1980. The role of the Akosombo Dam on the Volta river in causing coastal erosion in central and eastern Ghana (West Africa). *Marine Geology*, 37(4), 323-332.
- Masselink, G., Russell, P., Turner, I., and Blenkinsopp C., 2009. Net sediment transport and morphological change in the swash zone of a high-energy sandy beach from swash event to tidal cycle time scales. *Marine Geology*, 267, 18–35.
- Masselink, G., and Short, A., 1993. The Effect of Tide Range on Beach Morphodynamics and Morphology: A Conceptual Beach Model. *Journal of Coastal Research*, 9(3), 785-800.
- Plant, N. G., and Holman, R. A., 1997. Intertidal beach profile estimation using video images, *Marine Geology*, 140, 1-24.
- Puleo, J.A., Farquharson, G., Fraiser, S.J., and Holland, K.T., 2003. Comparison of optical and radar measurements of surf and swash zone velocity fields. *Journal of Geophysical Research*, 108(3), 3100-3112.
- Ruessink, B. G., Kuriyama, Y., Reniers, A. J. H. M., Roelvink, J. A., and Walstra, D. J. R., 2007. Modeling cross-shore sandbar behavior on the timescale of weeks. *Journal of Geophysical Research*, 112.
- Sagoe-Addy, K., and Appeaning Addo, K., 2013. Effect of predicted sea level rise on tourism facilities along Ghana's Accra coast. *Journal of Coastal Conservation and Management*. 17(1), 155-166.
- Smith, R. K., and Bryan, K. R., 2007. Monitoring beach face volume with a combination of intermittent profiling and video imagery. *Journal of Coastal Research*, 892-898.
- Sterl, A., and Caires, S., 2005. Climatology, variability and extrema of ocean waves- the web-based KNMI/ERA-40 Wave Atlas. *International Journal of Climatology*, 25, 963–977.
- Stive, M. J.F., Aarninkhof, S. G.J., Luc Hamm, Hanson, H., Larson, M., Wijnberg, K. M., Nicholls, R. J., and Capobianco, M., 2002. Variability of shore and shoreline evolution. *Coastal Engineering*, 47, 211–235.
- Stockdon, H.F., Sallenger, A.H., List, J.H. and Holman, R.A., 2002. Estimation of shoreline position and change using airborne topographic lidar data. *Journal of Coastal Research*, 18(3), 502–513.
- Stokes, C, Davidson, M., and Russell P., 2015. Observation and prediction of three-dimensional morphology at a high-energy macrotidal beach. *Geomorphology*, 243,1–13.
- The Wamdi Group, 1988. The WAM Model-A Third generation ocean wave prediction model. *Journal of Physical Oceanography*, 18, 1775–1810.
- Turner, I.L., and Leatherman, S.P., 1997, Beach Dewatering as a 'Soft' Engineering Solution to Coastal Erosion – History and Critical Review. *Journal of Coastal Research*, 13(4), 1050-1063.
- Wiafe G., Boateng I., Addo, A. K., Quashigah, P.N., Ababio S.D. and Laryea S. W., 2013. Handbook of Coastal Processes and Management in Ghana. *The Choir Press*, pp., 274.
- Wright, L.D., and Short, A.D., 1984. Morphodynamic variability of surf zones and beaches: A synthesis. *Marine Geology*, 56, 93-118.